Calcium-Induced Lateral Phase Separations in Phosphatidylcholine–Phosphatidic Acid Mixtures. A Raman Spectroscopic Study†

Rachid Kouaouci,‡ John R. Silvius,§ Ian Graham,∥ and Michel Pézolet*,‡

Département de chimie, Université Laval, Cité Universitaire, Québec, Canada G1K 7P4, and Departments of Biochemistry and Physics, McGill University, Montréal, Québec, Canada H3G 1Y6

Received April 30, 1985

ABSTRACT: The effects of calcium ions on mixed membranes of dimyristoylphosphatidic acid (DMPA) and dimyristoylphosphatidylcholine (DMPC) with either the PA or the PC component deuterated have been studied by Raman spectroscopy. The spectra of the pure components show that the acyl chains of hydrated DMPA bilayers are less tightly packed and have more trans bonds than those of DMPC. This behavior appears to be due to the particular arrangement of the polar head groups of DMPA for which the glycerol chain is oriented parallel to the bilayer surface. In agreement with the calorimetrically determined phase diagram [Graham, I., Gagné, J., & Silvius, J. R. (1985) *Biochemistry* (preceding paper in this issue)], the Raman results show that, in the absence of calcium, DMPA and DMPC are completely miscible at an equimolar ratio but undergo extensive phase separation in the presence of excess calcium. DMPC in phase-separated DMPC–DMPA (Ca^{2+}) mixtures has a conformation that is very similar to that of pure DMPC bilayers, but it is packed more tightly since, depending on the temperature, it is at least partly incorporated into either a solid solution in DMPA or a DMPA–Ca^{2+}-rich "cochleate" phase. This latter shows the same characteristics as the cochleate phase of pure DMPA–Ca^{2+} which is highly ordered and does not give rise to a thermotropic transition between 5 and 100 °C. However, the cochleate phase in DMPA (Ca^{2+})–DMPC mixtures contains some 20 mol % of DMPC trapped in small domains. These clusters do not melt cooperatively but become as fluid as pure DMPC at 50 °C.

In recent years, a particular interest has been manifested with regard to the role of calcium ions in many cellular processes such as nerve excitation and fusion of biological membranes (Poste & Allison, 1973). It is now well established that these divalent cations can induce drastic structural changes in model membranes composed of acidic phospholipids (Verkleij et al., 1974; Hauser & Shipley, 1984; Papahadjopoulos et al., 1975; Cullis et al., 1978) due to the anionic character of the polar head group of these lipids. In mixed systems containing zwitterionic and negatively charged phospholipids, membrane fusion (Papahadjopoulos & Poste, 1975; Düzgünes et al., 1984; Liao & Prestegard, 1979) or lateral phase separation (Jacobson & Papahadjopoulos, 1975; Van Dick et al., 1978; Galla & Sackmann, 1975; Ohnishi & Ito, 1974; Hui et al., 1983; Silvius & Gagné, 1984a,b; Graham et al., 1985) has been observed in the presence of Ca^{2+} ions using several physical techniques.

Vibrational spectroscopy is well suited for structural studies on biomembranes, since it provides direct information on the conformation of membrane constituents. For example, it has recently been shown that Raman spectroscopy can monitor simultaneously the conformation of the protein and phospholipid moieties of model membranes of charged phospholipids and basic proteins or polypeptides (Pézolet et al., 1982; Carrier & Pézolet, 1984; Faucon et al., 1983). Another interesting advantage of vibrational spectroscopy is the possibility of using phospholipids with fully deuterated acyl chains to investigate multicomponent systems. For binary mixtures of lipids with hydrogenated and deuterated chains, it is possible to monitor simultaneously the conformation of each component of the mixtures by looking at either the C–H or the C–D stretching regions. The usefullness of deuterated lipids in the study of model membrane systems has been clearly demonstrated by Raman spectroscopy (Mendelsohn & Tarashi, 1978; Mendelsohn & Maisano, 1978; Mendelsohn & Koch, 1980) and more recently by Fourier transform infrared spectroscopy (Mendelsohn et al., 1984).

To elucidate the ionotropic behavior of phospholipid mixtures, and to obtain more information on the phase separation process at the molecular level, we have used Raman spectroscopy to study the effect of Ca^{2+} ions on mixed membranes of dimyristoylphosphatidylcholine (DMPC)[1] and dimyristoylphosphatidic acid (DMPA), with either one of the lipids being deuterated. This constitutes the first study in which a deuterated lipid with a negatively charged polar head group is used. These results will be compared with those obtained calorimetrically on the same system.

Materials and Methods

Materials. The disodium salt of dimyristoylphosphatidic acid (DMPA) was purchased from Sigma Chemical Co. while dimyristoylphosphatidylcholine (DMPC) and its deuterated derivative (DMPC-d_{54}) were obtained from Avanti Polar Lipids Inc. These samples were used without further purification. Deuterated DMPA (DMPA-d_{54}) was prepared from DMPC-d_{54} as described for DMPA in the preceding paper

† This research was supported in part by the National Science and Engineering Research Council of Canada (M.P.), the Medical Research Council of Canada (J.R.S.), the Fonds FCAC, Province of Québec (M.P.), and the Fonds de la recherche en santé du Québec (J.R.S.).

‡ Département de chimie, Université Laval.

§ Department of Biochemistry, McGill University.

∥ Department of Physics, McGill University.

[1] Abbreviations: DMPC, dimyristoylphosphatidylcholine; DMPA, dimyristoylphosphatidic acid; DMPC-d_{54}, DMPC with perdeuterated acyl chains; DMPA-d_{54}, DMPA with perdeuterated acyl chains; EDTA, ethylenediaminetetraacetic acid; Tris, tris(hydroxymethyl)aminomethane; Tes, *N*-[tris(hydroxymethyl)methyl]-2-aminoethanesulfonic acid; $\Delta\nu$, bandwidth; HPLC, high-pressure liquid chromatography; PS, phosphatidylserine; DPPG, dipalmitoylphosphatidylglycerol.

0006-2960/85/0424-7132$01.50/0

(Graham et al., 1985), but the sample was purified by preparative thin-layer chromatography on silica gel G plates using 50:20:10:10:5 chloroform–acetone–methanol–acetic acid–water as the developing solvent. Throughout this purification, redistilled HPLC-grade chloroform and electronic-grade methanol were used.

Raman Measurements. Binary phospholipid mixtures were prepared by dissolving appropriate amounts of each component in chloroform–methanol (87:3 v/v) at 50 °C. After complete dissolution of the solid, the solvent was evaporated at 50 °C under nitrogen. Final traces of solvent were removed by pumping overnight in a vacuum desiccator.

Calcium-free samples were prepared by suspending with a vortex mixer appropriate amounts of dry lipid mixtures in 50 mM Tris-HCl, 70 mM NaCl, and 10 mM EDTA, pH 7.5. After an incubation period of 15 min at 50 °C, the pH of the dispersions (10% weight) was measured with a combination microelectrode (Microelectrodes Inc.) and adjusted to 7.5 if necessary. Samples were then transferred into a glass capillary cell (1.5-mm diameter), centrifuged with a hematocrit centrifuge, and subjected to several heating and cooling cycles through the transition temperature. Samples containing calcium were prepared according to the same procedure except that the lipid concentration was 10 mM and the buffer was 50 mM Tris-HCl, 70 mM NaCl, and 30 mM $CaCl_2$, pH 7.5. The calcium concentration was therefore 3 times that of the phospholipid.

Raman spectra were recorded with a computerized Spex Model 1400 double monochromator (Savoie et al., 1979) with a spectral resolution of 5 cm^{-1}. The monochromator was calibrated with a neon discharge lamp, and the frequencies cited later are believed to be accurate to ± 2 cm^{-1} for sharp peaks. Spectra were excited transversely with the 514.5- or the 488.0-nm line of a Spectra Physics Model 165 argon ion laser; the laser power at the sample was approximately 150 mW. Capillaries containing the samples were placed in a thermoelectrically regulated sample holder (Pézolet et al., 1983) whose temperature was monitored at ± 0.2 °C with a copper–constantan thermocouple. Spectra were recorded digitally with an integrating period of 2 s and a frequency increment of 1 cm^{-1} for the C–D stretching region (1950–2350 cm^{-1}) and 2 cm^{-1} for the C–H stretching region (2750–3050 cm^{-1}). Spectra were all corrected for a slight fluorescent background by subtracting appropriate polynomial functions, and those of deuterated samples were seven-point-smoothed by the algorithm of Savitsky & Golay (1967).

Calorimetric Measurements. Samples containing mixtures of hydrogenated and deuterated DMPA or DMPC were prepared for calorimetry as described in the previous paper (Graham et al., 1985) or by the methods described above for preparation of samples for Raman spectroscopy. In both cases, the final composition of the sample buffer was 70 mM NaCl, 50 mM Tris, and 10 mM EDTA, pH 7.5, or 70 mM NaCl, 50 mM Tris, and 30 mM $CaCl_2$, pH 7.5, and the final lipid concentration was 6 mM. However, in the former method, the samples were initially dispersed and equilibrated at this relatively dilute lipid concentration, while in the latter method, the lipids were first equilibrated at concentrations of lipid and calcium comparable to those used in the Raman experiments and then diluted with cold buffer just before calorimetry to give the final lipid and ion concentrations indicated above. The calorimetric behavior of samples prepared by either method was quite comparable in all cases.

Calorimetric measurements on these samples were obtained with a Microcal MC-1 high-sensitivity differential scanning calorimeter under the conditions described in the preceding paper (Graham et al., 1985).

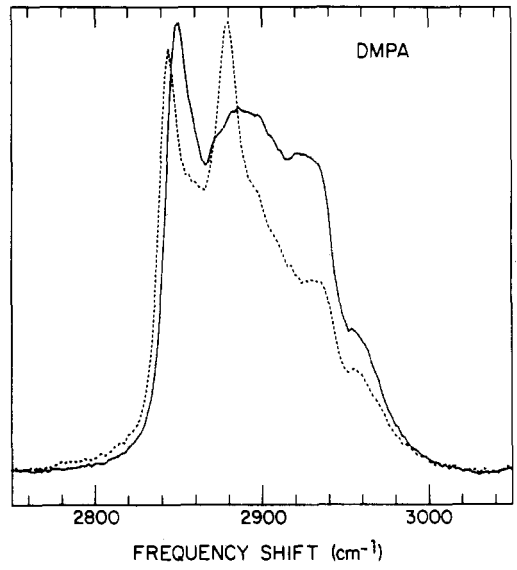

FIGURE 1: Raman spectra of a 10% (w/w) dispersion of DMPA at 20 °C (dotted line) and 60 °C (solid line).

RESULTS

Raman Spectra of Pure Lipid Components. Although Raman spectra of phospholipids contain several bands that are sensitive to the conformation of different parts of the phospholipid molecules, there is in binary systems a considerable overlapping of these bands between 500 and 1900 cm^{-1}. In order to eliminate as much as possible the spectral interferences, we have investigated in this study only the carbon–hydrogen and carbon–deuterium stretching regions, 2750–3050 and 1950–2350 cm^{-1}, respectively.

The Raman spectra of the carbon–hydrogen stretching region of a DMPA multilamellar dispersion in the gel and liquid-crystalline phases are reproduced in Figure 1. Even though this region is rather congested, it is nevertheless particularly sensitive to the molecular order in phospholipid bilayers. At low temperatures, this region is dominated by two strong bands at 2850 and 2880 cm^{-1} that are respectively assigned to the acyl chain methylene symmetric and antisymmetric stretching vibrations (Gaber & Peticolas, 1977). The weaker bands observed at approximately 2930 and 2954 cm^{-1} arise from the symmetric and asymmetric C–H stretching modes of terminal methyl groups, respectively (Spiker & Levin, 1975). For phosphatidylcholines, including DMPC-d_{54}, the choline group also contributes slightly to the scattering intensity in the C–H region around 2962 and 3041 cm^{-1}.

As seen in Figure 1, when the molecular order is decreased at higher temperature, the intensity of the 2930-cm^{-1} band increases. This change results in part from underlying infrared-active methylene asymmetric stretching modes that become Raman active when the chain symmetry is lowered (Bunow & Levin, 1977) and also from a change in the Fermi resonance between the symmetric C–H stretching mode of the terminal methyl groups and the first overtone of the asymmetric CH_2 bending mode (Hill & Levin, 1979). Simultaneously with the increase of the 2930-cm^{-1} band intensity, the 2880-cm^{-1} feature shifts to higher frequency, broadens, and decreases markedly in intensity. The latter change is partially due to the lowering of the intensity of the broad underlying background, which arises from inter- and intramolecular Fermi resonance interactions between the methylene symmetric C–H

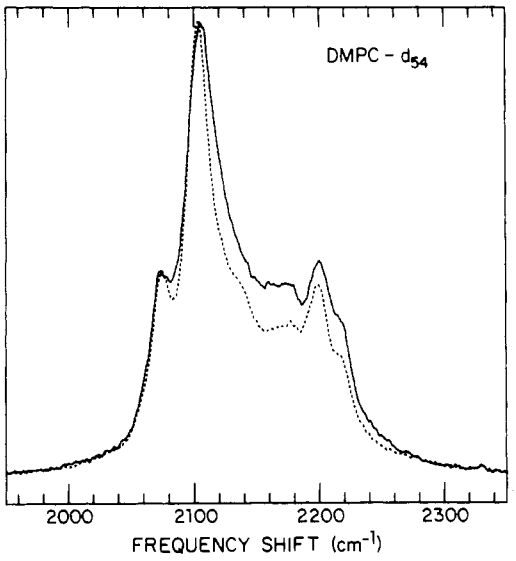

FIGURE 2: Raman spectra of a 10% (w/w) dispersion of DMPC-d_{54} at 10 °C (dotted line) and 40 °C (solid line).

stretching mode and the different binary combinations of the methylene bending fundamental (Snyder et al., 1978; Snyder & Scherrer, 1979). The broadening of the 2880-cm^{-1} band depends on several factors such as conformational disorder (Snyder et al., 1978) and chain rotational mobility (Snyder et al., 1980).

To follow the effect of temperature on the molecular order in pure or mixed bilayers, the h_{2880}/h_{2850} and h_{2930}/h_{2880} peak height intensity ratios were used. Both ratios monitor essentially the overall disorder of the lipid acyl chain matrix, but the h_{2880}/h_{2850} ratio is in addition a sensitive probe of the intermolecular vibrational coupling and the lateral packing of the acyl chains. These ratios were determined by computer according to the following procedure. First, a straight base line was drawn from 2760 to 3020 cm^{-1}, and the background was subtracted. The maximum heights of the 2850- and 2880-cm^{-1} bands were then determined as averages of three data points around the maxima. Since the maximum of the 2930-cm^{-1} band was not always evident, the intensity of this component was always taken as the spectral intensity at 2925 cm^{-1}. With this procedure, these ratios were very reproducible.

The spectral region due to the carbon–deuterium stretching vibrations of DMPC-d_{54} below and above the gel to liquid-crystalline phase transition is shown in Figure 2. The main feature in this region is the 2103-cm^{-1} band assigned to the CD_2 symmetric stretching mode (Mendelsohn et al., 1976). In addition, several weaker bands due to the CD_2 asymmetric stretch, at 2177 cm^{-1}, and to CD_3 vibrations, at 2076, 2125, and 2213 cm^{-1}, are also observed (Bryant et al., 1982).

As the DMPC-d_{54} dispersion undergoes the gel to liquid-crystalline phase transition, the line width of the 2103-cm^{-1} band increases markedly. From isotopic dilution experiments, Mendelsohn & Koch (1980) have demonstrated that the half-width of this feature, measured from a base line between 2060 and 2240 cm^{-1}, is not related to interchain vibrational coupling and reflects essentially the formation of gauche bonds along the acyl chains. Later, Bryant et al. (1982) have proposed that the line width of the 2103-cm^{-1} band can monitor either lateral interactions or gauche rotamer formation, depending on the height at which it is measured from a straight base line between 2000 and 2300 cm^{-1}.

In the present study, we have recorded the C–D stretching region from 1950 to 2350 cm^{-1} in order to clearly define the base line. The line width of the band due to the CD_2 symmetric stretching mode was then determined at different heights from the baseline by using the algorithm of Cameron et al. (1982). The line width at 50% height ($\Delta\nu_{0.50}$) is highly sensitive to the lipid physical state, increasing from 32 to 47 cm^{-1} through the gel to liquid-crystalline phase transition of DMPC-d_{54}. However, in the temperature profiles obtained with this parameter, there was a significant scattering of the data points, and the plateau before the transition was not well-defined. This was most likely due to the presence of a weak shoulder assigned to a combination mode involving a C–C stretching fundamental (Bryant et al., 1982). To eliminate this problem, we have measured the line width at 65% of the peak height intensity ($\Delta\nu_{0.65}$), and the results were then very reproducible. In addition, we have observed by dissolving perdeuterated hexadecane in normal hexadecane that $\Delta\nu_{0.65}$ is insensitive to intermolecular chain interactions throughout the whole range of concentrations. Therefore, $\Delta\nu_{0.65}$ monitors mainly the gauche rotamer population.

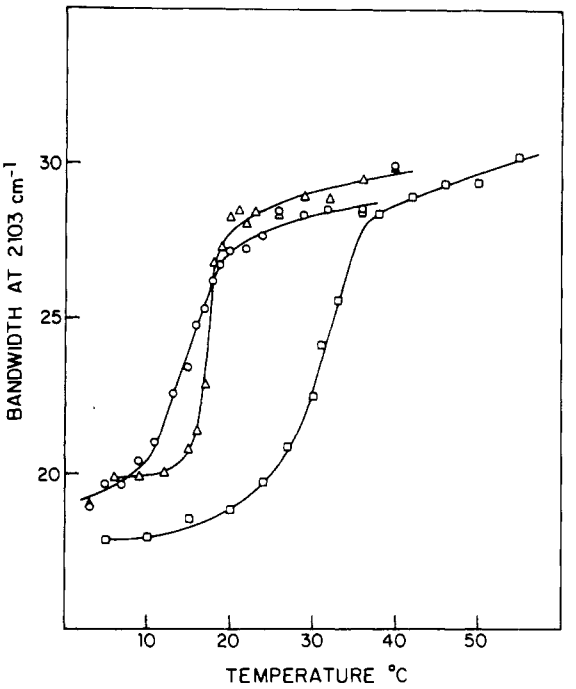

FIGURE 3: Temperature profiles of DMPC-d_{54} derived from the bandwidth at 65% of the height of the 2103-cm^{-1} Raman band: pure DMPC-d_{54} dispersion (Δ); equimolar DMPC-d_{54}–DMPA mixture in the absence (□) and in the presence (○) of calcium ions.

Thermotropic Behavior of an Equimolar Mixture of DMPA and DMPC-d_{54}. As seen in Figures 3 and 5, the temperature profile derived from $\Delta\nu_{0.65}$ of the 2103-cm^{-1} band in the Raman spectrum of a pure DMPC-d_{54} multilamellar dispersion and the corresponding calorimetric thermogram both display a transition at 18 °C. This 6 °C shift from the transition temperature (24 °C) of normal DMPC (Mabrey & Sturtevant, 1976) is in good agreement with previous results of Petersen et al. (1975) showing that perdeuteration of the acyl chains of phosphatidylcholines causes a 4–5 °C decrease of their phase transition temperature.

In Figure 4, the temperature dependence of the h_{2930}/h_{2890} and h_{2880}/h_{2850} intensity ratios for a multilamellar dispersion of DMPA at pH 7.5 is presented. As with pure DMPC-d_{54}, there is good agreement between the Raman results and the calorimetric ones (Figure 5). However, the gel to liquid-crystalline transition is observed at 45 °C which is approximately 4 °C lower than the published value for DMPA at pH 7.5 (Copeland & Andersen, 1982). On the other hand, previous work (Graham et al., 1985) showed that when DMPA

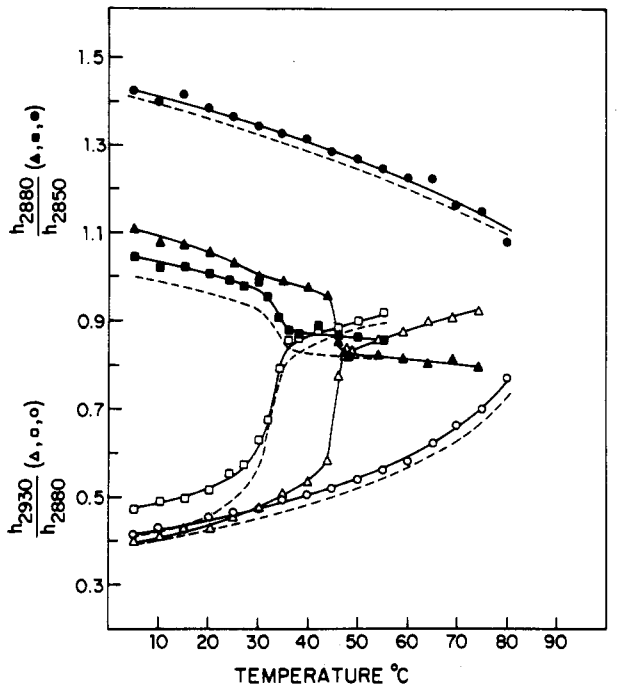

FIGURE 4: Temperature profiles of DMPA derived from the Raman spectral h_{2930}/h_{2880} (open symbols) and h_{2880}/h_{2850} (closed symbols) peak height intensity ratios: pure DMPA dispersion (Δ); equimolar DMPC-d_{54}–DMPA mixture in the absence (□) and in the presence (○) of calcium ions. The dashed lines represent the profiles after correction for the contribution from the nondeuterated choline group of DMPC-d_{54}.

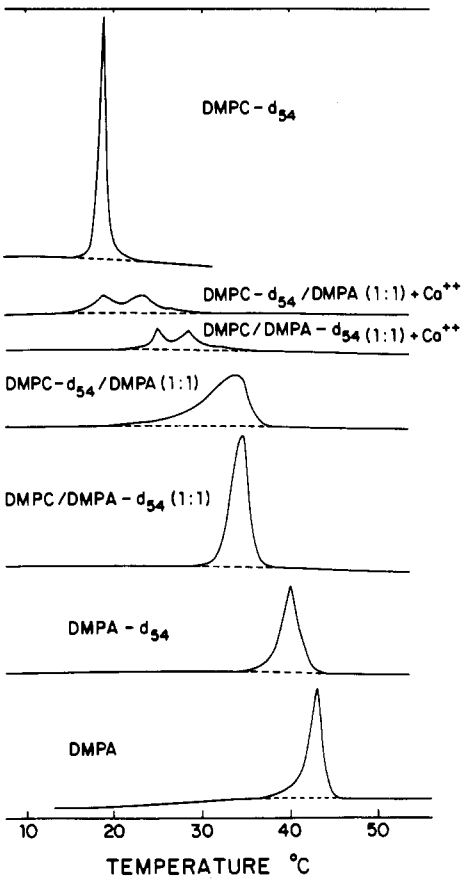

FIGURE 5: High-sensitivity differential scanning calorimetry thermograms recorded for different samples of hydrogenated and deuterated DMPC and DMPA. Details of sample preparation and equilibration are described under Materials and Methods.

from the same lot was dispersed in a different buffer, containing Tes–histidine instead of Tris, the calorimetric transition was detected at 49 °C. The different behavior of DMPA in the two buffers appears to be only a consequence of the replacement of histidine and Tes by Tris in the buffer system used here (unpublished observations).

Graham et al. (1985) have shown that at a 1:1 molar ratio DMPC and DMPA are completely miscible in the absence of divalent cations but undergo phase separation in the presence of an excess of calcium ions. We first studied the thermotropic behavior of an equimolar mixture of DMPC-d_{54} and DMPA in the absence of calcium. Raman spectroscopic results obtained for this mixture and for the pure lipid components are reproduced in Figures 3 and 4. The strong similarity between temperature profiles derived from either the DMPC-d_{54} or the DMPA component of the 1:1 mixture demonstrates unambiguously that the lipids are completely miscible at this concentration and that the spectral parameters used to determine these profiles are not subject to artifacts. As observed by calorimetry, equimolar mixtures of DMPA and DMPC-d_{54} melt over a 10 °C temperature range (Figure 5), and the transition midpoint temperature is close to the average of the transition temperatures of pure DMPA and DMPC-d_{54}.

As seen in Figure 3, the bandwidth of the 2103-cm^{-1} band of DMPC-d_{54} in the gel phase decreases significantly when this lipid is mixed with DMPA. This narrowing most likely results from the fact that the polar head group of DMPA is smaller than that of DMPC, allowing the acyl chains to pack more closely, with a correspondingly higher fraction of trans bonds, even though DMPA is charged at pH 7.5. This finding is also confirmed by comparing the C–C stretching mode regions in the spectra of normal DMPC and DMPA (unpublished results). On the other hand, in the liquid-crystalline phase, the intramolecular order of DMPC-d_{54} is the same as in the equimolar mixture (Figure 3).

To compare temperature profiles obtained from the C–H stretching region in the spectra of mixed DMPA–DMPC-d_{54} bilayers with those of pure DMPA dispersions, the intensity ratios have to be corrected to eliminate the contribution to the C–H region scattering intensity from the nondeuterated choline groups of DMPC-d_{54}. The choline group also gives rise to a well-separated band at 3041 cm^{-1} due to the asymmetric C–H stretching fundamental (Spiker & Levin, 1975). Since this band is absent in the spectrum of DMPA, it can be used as an internal intensity standard to correct the spectra of mixtures in the C–H region for the contribution of the choline group. The result of such a correction is shown in Figure 4. At equivalent temperature intervals below or above the phase transition temperature, the corrected values for the h_{2930}/h_{2880} ratio of the equimolar mixture of DMPA and DMPC-d_{54} are the same as for pure DMPA. Therefore, the chain order in the bilayers is quite similar. On the other hand, the h_{2880}/h_{2850} ratio in the gel phase is smaller for the mixture than for pure DMPA bilayers. As discussed above, this ratio is very sensitive to intermolcular vibrational coupling so that its lower values in the mixture might be due either to the isotopic dilution of the acyl chain or to a larger spacing of the acyl chains caused by the bulky head group of DMPC. As we will see later, the former explanation is the more likely one. In the liquid-crystalline state, the h_{2880}/h_{2850} ratio is the same for both the mixture and pure DMPA which is in good agreement with the results of Figure 3.

The addition of an excess of calcium ions to an equimolar dispersion of DMPA and DMPC-d_{54} perturbs drastically the thermotropic behavior of this mixture, as shown in Figures 3

and 4. As opposed to the results obtained in the absence of calcium, the Raman temperature profiles are completely different for each component of the mixture, suggesting that lateral phase separation has occurred. The PC component still gives rise to a phase transition, but this now occurs at a temperature that is approximately 15 °C lower than that of the calcium-free mixture and very close to that of the pure lipid (Figure 3). However, the transition of the phase-separated PC is broader than that of the pure lipid. By comparing Raman results with the calorimetric ones [Figure 5 and Graham et al. (1985)], this phenomenon can be readily explained. The thermogram for an equimolar DMPA–DMPC-d_{54} mixture in the presence of an excess of calcium shows two overlapping transitions, one due to the melting of the nearly pure phase-separated DMPC-d_{54}, and the second corresponding to the crossing of a line of three-phase coexistence in the phase diagram. Since the number of data points on the Raman temperature profiles are limited, the two transitions appear as a single broad one. Curiously, the onset of the Raman transition of the DMPC-d_{54} component is about 5 °C lower than the onset of the calorimetric transition. When the Raman experiment was repeated at a lipid concentration comparable to that used in the calorimetric experiments (6 instead of 10 mM) and using the calorimetric procedure, the Raman temperature profile obtained for the DMPC-d_{54} component agreed well with the calorimetric results for this mixture. However, at the low lipid concentration used in this experiment, the data points in the temperature profile showed appreciable scatter due to a poor signal to noise ratio in the original spectra. The difference observed between the Raman and calorimetric experiments with this system thus appears to simply result from the higher lipid concentration required for Raman spectroscopy. Such discrepancies were not observed with any of the other types of samples studied by the two techniques.

Above the transition temperature, the width of the 2103-cm^{-1} band of DMPC-d_{54} for the mixture in the presence of calcium is also smaller than that of the pure lipid. We believe that this is due to the fact that the Raman signal for DMPC-d_{54} comes from the totality of the PC present in the PA(Ca^{2+})–PC mixture, a significant amount of which is incorporated into phase-separated domains rich in PA–Ca^{2+} (Graham et al., 1985). As seen in Figure 4 from the C–H region, these domains are highly ordered since they give Raman spectra with a very high h_{2880}/h_{2850} ratio and do not exhibit any thermotropic transition from 5 to 80 °C. In fact, the profiles derived from the C–H region for the mixture in the presence of calcium are very similar to those obtained for pure DMPA–Ca^{2+} (Figure 6). The main difference is that the h_{2930}/h_{2880} ratio is always higher for the phase-separated PA-Ca^{2+} in the mixed bilayers than for pure DMPA–Ca^{2+} since the PA-Ca^{2+} domains in the former case incorporated 20 mol % PC (Graham et al., 1985). Therefore, even though there is not any distinct band that would indicate the presence of the cochleate phase unambiguously, the high value of the h_{2880}/h_{2850} ratio for the phase-separated PA–Ca^{2+} shows that, even when mixed with phosphatidylcholines, DMPA seems to form in the presence of calcium an ordered cochleate phase as for pure DMPA–Ca^{2+} (Liao & Prestegard, 1981; Van Dijck et al., 1978). The PC trapped in this phase does not melt at its normal transition temperature, and the bandwidth of the 2103-cm^{-1} band remains narrow.

Thermotropic Behavior of an Equimolar Mixture of DMPA-d_{54} and DMPC. In order to support the results obtained with the equimolar mixture of DMPC-d_{54} and DMPA,

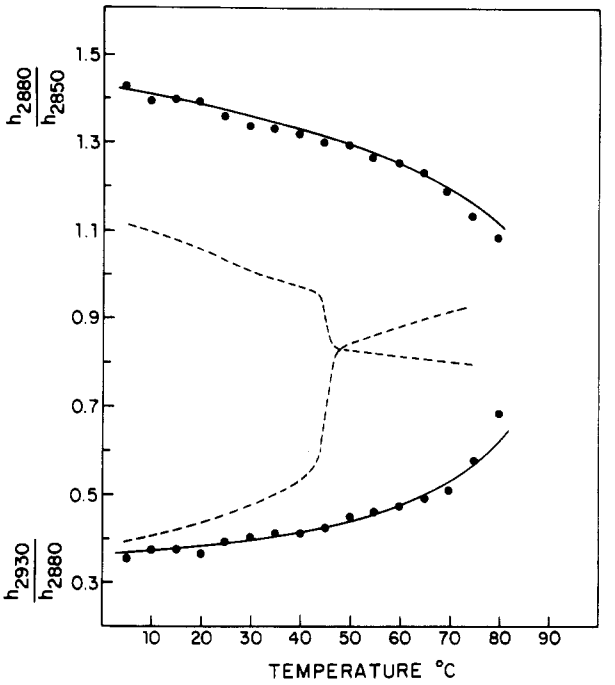

FIGURE 6: Temperature profiles of DMPA–Ca^{2+} complexes (1:1 molar ratio) derived from the Raman spectra h_{2930}/h_{2880} and h_{2880}/h_{2850} peak height intensity ratios. The dashed lines are for a pure DMPA dispersion prepared without Ca^{2+}.

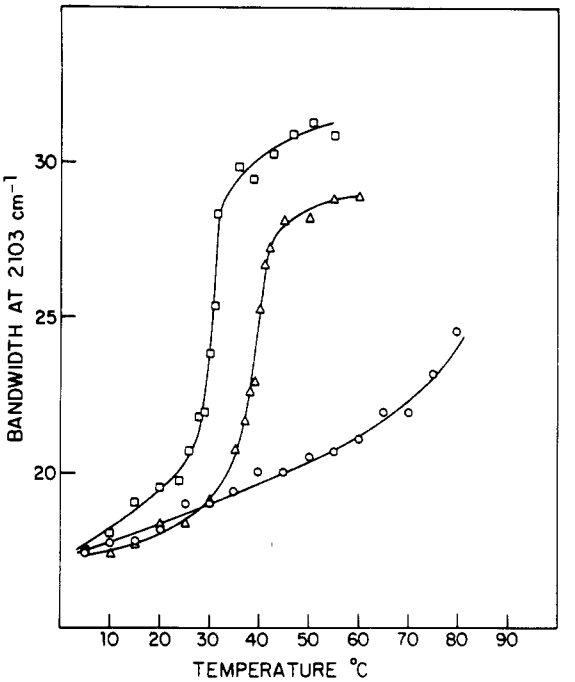

FIGURE 7: Temperature profiles of DMPA-d_{54} derived from the bandwidth at 65% of the height of the 2103-cm^{-1} Raman band: pure DMPA-d_{54} dispersion (Δ); equimolar DMPC–DMPA-d_{54} mixture in the absence (□) and in the presence (○) of calcium ions.

we have also investigated the thermotropic behavior of an equimolar mixture of deuterated phosphatidic acid and hydrogenated phosphatidylcholine. The Raman results for this mixture are shown in Figures 7 and 8 while the calorimetric results are shown in Figure 5. In general, the qualitative agreement between these results and those obtained with the DMPC-d_{54}–DMPA mixture is quite good, reinforcing the conclusions drawn from the preceding section. However, some special features of the results obtained with these mixtures

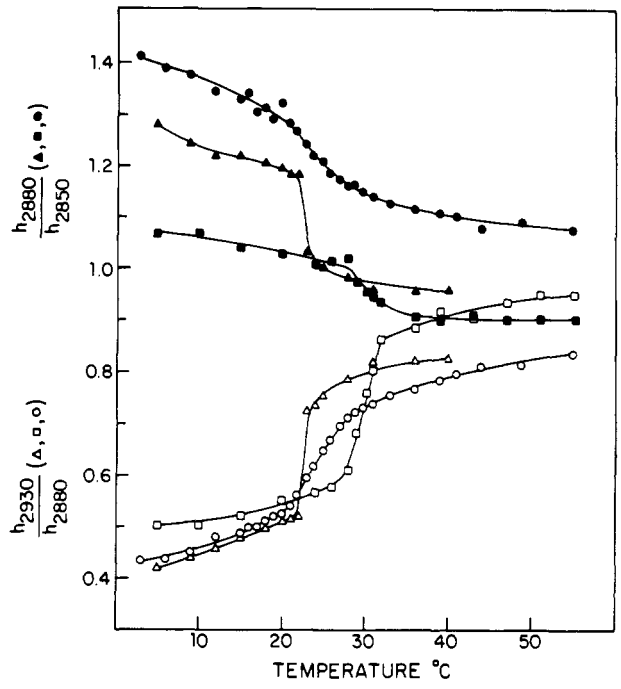

FIGURE 8: Temperature profiles of DMPC derived from the Raman spectral h_{2930}/h_{2880} (open symbols) and h_{2880}/h_{2850} (closed symbols) peak height intensity ratios: pure DMPC dispersion (Δ); equimolar mixture of DMPC–DMPA-d_{54} in the absence (□) and in the presence (○) of calcium ions.

provide further information on the behavior of the PA–PC system, as discussed below.

The comparison between the Raman results of Figures 3 and 4 and Figures 6–8 reveals a remarkable correspondence between the temperature profiles obtained from DMPC-d_{54}–DMPA and DMPC–DMPA-d_{54} equimolar mixtures in the absence of calcium ions. For example, at 10 °C, the h_{2930}/h_{2880} ratio is equal to 0.49 for DMPC-d_{54}–DMPA as compared to 0.51 for DMPC–DMPA-d_{54}. Similarly, the bandwidth of the 2103-cm^{-1} feature of the deuterated moiety is 18 cm^{-1} in the spectra of both mixtures at 10 °C. The only discrepancy in the results is for the fluid phase where the mixture made with deuterated DMPA seems to be slightly more disordered. Therefore, the spectral parameters used throughout this study appear independent of the nature of the phospholipid head groups per se but are only sensitive to the acyl chain conformation or to the chain packing characteristics.

The width of the 2103-cm^{-1} band in the spectra of pure DMPC-d_{54} and DMPA-d_{54} (Figures 3 and 7, respectively) confirms our previous findings that the acyl chains of DMPA in the gel state have more trans bonds while the chain conformation is the same for both lipids in the liquid-crystalline state. For the DMPC–DMPA-d_{54} mixture after calcium-induced phase separation, the DMPA-d_{54} component no longer shows a phase transition. Between 5 and 30 °C, the bandwidth of the 2103-cm^{-1} feature in its Raman spectrum is very close to that of pure DMPA-d_{54} in the gel state.

The curves constructed from the h_{2880}/h_{2850} spectral index for pure DMPC (Figure 8) and DMPA (Figure 4) show that whether the bilayers are in the gel or in the liquid-crystalline states, this intensity ratio is always much higher for DMPC. On the other hand, at equivalent temperature intervals below and above the transition temperatures of DMPA and DMPC, the h_{2930}/h_{2880} ratio has essentially the same value for the two lipids. Examination of the spectra of DMPA and DMPC in the gel state shows that for DMPC the 2850-cm^{-1} band is much broader and therefore weaker in intensity. As noted by Snyder et al. (1978), the broadening of the 2850-cm^{-1} feature is associated with higher intermolecular interactions between neighboring acyl chains, suggesting that the acyl chains interact more strongly in DMPC than in DMPA multilayers. However, the C–D and C–C stretching mode regions (data not shown) show that the number of trans bonds is slightly higher for DMPA than for DMPC.

The crystal structures of DMPC and DMPA have already been determined by X-ray crystallography by Pearson & Pascher (1979) and Harlos et al. (1984), respectively. There are three major structural differences between the two lipids. First, for DMPA, the glycerol chain is parallel to the bilayer surface instead of being roughly perpendicular as in DMPC. Second, because of its particular glycerol orientation and to ensure the parallel packing of the hydrocarbon chains, DMPA has a bend in the γ chain instead of the β chain. Third, in DMPA, the phosphate groups pack with a rather small cross section which leads to the partial interdigitation of the phosphate groups of adjacent bilayers and to a close packing of the acyl chains. Our Raman results are in very good agreement with the X-ray data since the h_{2880}/h_{2850} intensity ratio has a value of 1.63 for solid DMPA compared to 1.35 for solid DMPC (unpublished observations), thus indicating that the hydrocarbon chains of solid DMPA interact more strongly. When dispersed in water, the situation is reversed. According to Harlos et al. (1984), because of the peculiar arrangement of the polar head group of DMPA, the water molecules act as spacer molecules into the polar group region during hydration of the lipid. Therefore, the difference in the hydration of DMPA and DMPC is likely at the origin of the lower value of the h_{2880}/h_{2850} intensity ratio for hydrated DMPA. In addition, since the glycerol backbone of DMPA is parallel to the bilayer surface, bending of the γ chain is not necessary if the chains are not tightly packed for hydrated DMPA bilayers. In fact, the carbonyl stretching mode region in the Raman spectrum of a 10% (w/w) dispersion of DMPA in water (data not shown) displays a relatively sharp C=O band at 1740 cm^{-1} with a shoulder on the low-frequency side. According to the assignment of the C=O region proposed by Levin et al. (1982), this would indicate that the C_1–C_2 bonds of the γ and β chains of DMPA are nearly in the trans conformation. Thus, for hydrated DMPA, the particular orientation of the glycerol chain and the spacing between the lipid molecules favor the all-trans conformation of the two hydrocarbon chains below the phase transition temperature.

When DMPC is mixed with DMPA-d_{54}, the resulting decrease of the h_{2880}/h_{2850} ratio, particularly in the gel-state temperature domain (Figure 8), is much larger than that detected when DMPC-d_{54} is mixed with DMPA (Figure 4). We believe that the marked diminution of this spectral intensity ratio for DMPC on mixing with DMPA-d_{54} is due to a simultaneous decrease of the 2880-cm^{-1} band, caused by the reduction of the underlying Fermi resonance background because of isotopic dilution, and an increase in the intensity of the 2850-cm^{-1} feature, due to weaker intermolecular vibrational coupling. The latter effect is confirmed by the narrowing of this band. For DMPA–DMPC-d_{54} mixtures, the two effects act in opposite directions so that the lowering of the h_{2880}/h_{2850} ratio is smaller. The low intensity of the 2880-cm^{-1} band in the spectrum of the DMPC–DMPA-d_{54} mixture also affects the h_{2930}/h_{2880} ratio, which becomes higher than that of pure DMPC dispersions over the whole temperature profile.

As for DMPC-d_{54}–DMPA mixtures, calcium ions induce extensive lateral phase separation in mixed DMPC–DMPA-d_{54}

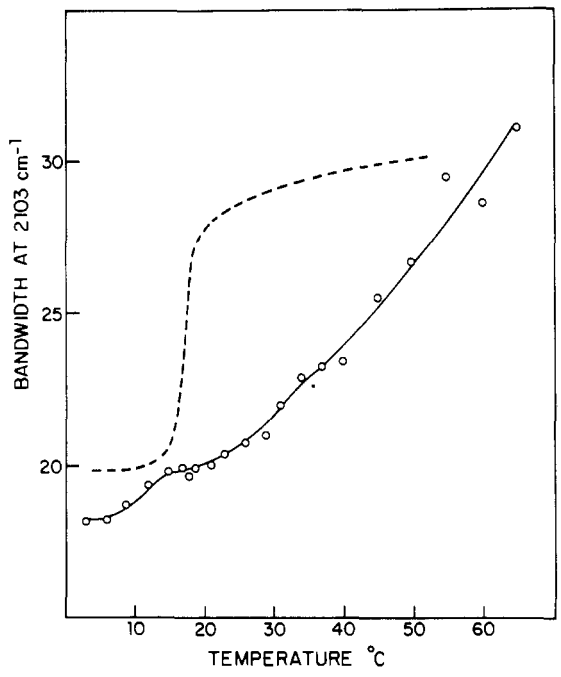

FIGURE 9: Behavior of the bandwidth at 65% of the height of the 2103-cm^{-1} Raman band of DMPC-d_{54} at 25 mol % in DMPA in the presence of calcium ions. The dashed curve is for pure DMPC-d_{54}.

bilayers (Figures 5 and 8). Below the transition, the h_{2930}/h_{2880} spectral index is the same for both DMPC and DMPA in the phase-separated PA(Ca^{2+})–PC mixtures and for pure DMPC. Above the transition, this ratio is slightly smaller for the mixed system. The h_{2880}/h_{2850} ratio of DMPC is always much higher after phase separation, reflecting strong intermolecular vibrational coupling.

Thermotropic Behavior of a 1:3 DMPC-d_{54}–DMPA Mixture in the Presence of Calcium. According to the phase diagram of DMPC–DMPA in the presence of calcium ions (Graham et al., 1985), at 25 mol % DMPA the major part of this lipid is incorporated into the PA–Ca^{2+}-rich phase. The effect of temperature on the bandwidth of the 2103-cm^{-1} feature in the spectrum of trapped DMPC-d_{54} is presented in Figure 9. As seen in this figure, no significant cooperative thermotropic transition is observed between 5 and 60 °C. Instead, there is a gradual increase of the $\Delta\nu_{0.65}$ parameter as the temperature is raised. At 5 °C, the bandwidth is slightly smaller than for pure DMPC-d_{54}, but at 50 °C, it is almost the same.

Discussion

The results presented here on DMPA and DMPC mixtures clearly demonstrate the potential of Raman spectroscopy to study phospholipid miscibility and calcium-induced lateral phase separation. The use of lipid mixtures in which one component has deuterated acyl chains provides the unique advantage of being able to monitor simultaneously and without using any perturbing probe the conformation and the chain packing characteristics of each lipid in the mixture. In addition, besides being a very useful technique to follow phospholipid thermotropic phase transition, Raman spectroscopy can also provide valuable structural information on certain phases like the cochleate one that is not accessible by differential scanning calorimetry.

In agreement with the calorimetric investigation of mixtures of DMPC and DMPA (Van Dijck et al., 1978; Graham et al., 1985), the Raman and calorimetric results presented above show that DMPC-d_{54}–DMPA and DMPC–DMPA-d_{54} mixtures are completely miscible at an equimolar ratio in the absence of divalent cations but undergo extensive phase separation in the presence of calcium ions. The latter phenomenon has previously been reported for other PA–PC mixtures using several techniques such as electron spin resonance, X-ray diffraction, freeze–fracture electron microscopy, and scanning calorimetry (Ohnishi & Ito, 1974; Galla & Sackman, 1975; Caffrey & Feigenson, 1984; Hartmann et al., 1977; Verkleij et al., 1982).

The temperature profiles obtained from the Raman spectra for the PA-rich phase provide conclusive evidence that Ca^{2+} induces a major reorganization of the PA component into a highly ordered phase like the cochleate one reported for phosphatidylserine–Ca^{2+} (Papahadjopoulos et al., 1975). It is interesting at this point to compare the DMPA–Ca^{2+}-rich phase in phase-separated PA(Ca^{2+})–PC bilayers with that of pure DMPA–Ca^{2+}. As shown in Figure 6, the pure DMPA–Ca^{2+} complex displays a Raman spectrum with a low h_{2930}/h_{2880} intensity ratio and a very high h_{2880}/h_{2850} spectral index, thus indicating that the lipid acyl chains are packed very tightly and give rise to high intermolecular vibrational coupling. In addition, neither of the intensity ratios shows that the acyl chains undergo any distinct thermotropic transition between 5 and 80 °C. These results are in very good agreement with the electron spin resonance results of Ito & Ohnishi (1974) which show that calcium causes a reduction of the mobility of the acyl chains of natural PA derived from egg PC and induces a closer packing of the phospholipid molecules. In addition, our results agree well with those obtained by Raman spectroscopy on the effect of Ca^{2+} on bovine brain PS (Hark & Ho, 1979, 1980) and DPPG (Susi, 1981) and by infrared spectroscopy on the properties of PS–Ca^{2+} complexes (Dluhy et al., 1983). All complexes of anionic lipids and calcium studied so far by vibrational spectroscopy exhibit acyl chains that are highly ordered and in the all-trans conformation. In addition, infrared spectroscopy shows that Ca^{2+} binds to the PS phosphate as a bidentate ligand and causes a dehydration of the phosphate ester (Dluhy et al., 1983).

On the whole, the temperature profiles obtained from the Raman spectra of the DMPA-rich phase produced after addition of calcium ions to an equimolar DMPC-d_{54}–DMPA mixture are very similar to those of pure DMPA–Ca^{2+}. The profiles derived from the h_{2880}/h_{2850} ratio are essentially superimposable for the two systems while the h_{2930}/h_{2880} ratio is always higher for the phase-separated PA–Ca^{2+} than for pure DMPA–Ca^{2+}. Therefore, the interchain interactions and probably the level of hydration are the same for the two phases, but PA–Ca^{2+} is more disordered when in the mixed PA-(Ca^{2+})–PC system. Since pure DMPC bilayers are also more disordered than the cochleate phase of DMPA–Ca^{2+}, we believe that the DMPC incorporated in the PA–Ca^{2+}-rich phases is at the origin of the slight disordering of this phase in the mixed system.

We may then question about the structure or the molecular organization of the DMPC trapped in bilayers rich in PA–Ca^{2+}. As seen in Figure 9, the PC component in the mixture does not give rise to a significant cooperative transition but rather melts very slowly as the temperature is raised. At the onset of the temperature profile, the DMPC in the cochleate phase has more trans bonds than pure DMPC at the same temperature, but at 50 °C, they display the same intramolecular order. On the other hand, comparison of Figures 7 and 9 shows that the DMPC molecules in the cochleate phase melt more rapidly than the PA molecules in this phase, since at 50 °C the width of the band due to the CD_2 symmetric

stretching mode of DMPC-d_{54} incorporated in the cochleate phase has a value of 27 cm^{-1} compared to 20 cm^{-1} for the DMPA–Ca^{2+}-rich phase. Therefore, the DMPC molecules are not uniformly distributed in the cochleate phase but are rather clustered. Since these domains do not melt cooperatively, they either are heterogeneous in size or are very small.

The phase diagram for the DMPC–DMPA system in the presence of calcium ions (Graham et al., 1985) shows that at a lipidic equimolar ratio and at low temperature, domains of essentially pure DMPC are in equilibrium with a solid solution containing approximately 75 mol % DMPA. According to our Raman results, the acyl chains of the DMPC component in DMPA(Ca^{2+})–DMPC bilayers and in pure DMPC bilayers have the same conformation below the phase transition temperature (Figures 3 and 8). Therefore, it seems that the conformation of the DMPC chains for the solid solution is equivalent to that of pure DMPC in the gel state. However, the h_{2880}/h_{2850} intensity ratio (Figure 8) reveals that the intermolecular vibrational coupling of the acyl chains of DMPC is much stronger in the DMPA–DMPC bilayers after addition of calcium. We believe that this strong interchain interaction is due to the presence of domains of the solid DMPC–DMPA solution in such bilayers and also to the partial dehydration of the system after addition of calcium ions. At 10 °C, the h_{2880}/h_{2850} ratio is essentially the same for the DMPC and DMPA components of PA(Ca^{2+})–PC mixtures (compare Figures 4 and 8) and slightly lower for the solid phase of pure DMPC. After the complete decomposition of the solid solution at higher temperatures, in DMPA(Ca^{2+})–DMPC mixtures, nearly pure DMPC in the liquid-crystalline state coexists with the DMPA–Ca^{2+}-rich cochleate phase. The Raman spectra for the PC component under these conditions show that the acyl chains are still quite close together, although the packing is looser than for the DMPA(Ca^{2+})-rich phase, and have more trans bonds than pure DMPC in the fluid state (Figures 3 and 8). Both observations correlate quite well with the fact that DMPC in the liquid-crystalline state contains some 10 mol % of DMPA and is in equilibrium with the cochleate phase in which are trapped domains of DMPC.

In summary, the Raman results are in very good agreement with the calorimetrically determined phase diagram (Graham et al., 1985) which shows that calcium ions induce extensive lateral phase separation in DMPA–DMPC mixtures. Phase-separated DMPC has a conformation that is very similar to but more closely packed than that of pure DMPC bilayers. The DMPA(Ca^{2+}) rich phase has essentially the same characteristics as pure DMPA(Ca^{2+}), but it contains DMPC which tends to form clusters within this phase. However, these clusters do not give rise to any cooperative thermotropic transition.

Registry No. DMPC, 18194-24-6; DMPA, 28874-52-4; DMPA-d_{54}, 98482-22-5; Ca, 7440-70-2.

References

Bryant, G. L., Lavialle, F., & Levin, I. W. (1982) *J. Raman Spectrosc. 12*, 118–121.

Bunow, M., & Levin, I. W. (1977) *Biochim. Biophys. Acta 487*, 388–394.

Caffrey, G. W., & Feigenson, G. W. (1984) *Biochemistry 23*, 323–331.

Cameron, D. G., Kauppinen, J., Moffatt, D., & Mantsch, H. H. (1982) *Appl. Spectrosc. 36*, 245–250.

Carrier, D., & Pézolet, M. (1984) *Biophys. J. 46*, 497–506.

Copeland, B. R., & Andersen, H. C. (1982) *Biochemistry 21*, 2813–2820.

Cullis, P. R., van Dick, P. W. M., de Kruijff, B., & de Gier, J. (1978) *Biochim. Biophys. Acta 513*, 21–30.

Dluhy, R. A., Cameron, D. G., Mantsch, H. H., & Mendelsohn, R. (1983) *Biochemistry 22*, 6318–6325.

Düzgünes, N., Paiement, J., Freeman, K. B., Lopez, N. G., Wilschut, J., & Papahadjopoulos, D. (1984) *Biochemistry 23*, 3486–3494.

Faucon, J. F., Dufourcq, J., Bernard, F., Duchesneau, L., & Pézolet, M. (1983) *Biochemistry 22*, 2179–2185.

Gaber, B. P., & Peticolas, W. L. (1977) *Biochim. Biophys. Acta 465*, 260–274.

Galla, H. J., & Sackmann, E. (1975) *Biochim. Biophys. Acta 401*, 509–529.

Graham, I., Gagné, J., & Silvius, J. R. (1985) *Biochemistry* (preceding paper in this issue).

Hark, S.-K., & Ho, J. T. (1980) *Biochim. Biophys. Acta 601*, 54–62.

Harlos, K., Eibl, H., Pascher, I., & Sundell, S. (1984) *Chem. Phys. Lipids 34*, 115–126.

Hartmann, W., Galla, H. J., & Sackmann, E. (1977) *FEBS Lett. 78*, 169–172.

Hauser, H., & Shipley, G. G. (1984) *Biochemistry 23*, 34–41.

Hill, I. R., & Levin, I. W. (1979) *J. Chem. Phys. 70*, 842–851.

Hui, S. W., Boni, L. T., Stewart, T. P., & Isac, T. (1983) *Biochemistry 22*, 3511–3516.

Ito, T., & Ohnishi, S. I. (1974) *Biochim. Biophys. Acta 352*, 29–37.

Jacobson, K., & Papahadjopoulos, D. (1975) *Biochemistry 14*, 152–161.

Levin, I. W., Mushayakarara, E., & Bittman, R. (1982) *J. Raman Spectrosc. 13*, 231–234.

Liao, M. J., & Prestegard, J. H. (1979) *Biochim. Biophys. Acta 550*, 157–173.

Liao, M. J., & Prestegard, J. H. (1981) *Biochim. Biophys. Acta 645*, 149–156.

Mabrey, S., & Sturtevant J. M. (1976) *Proc. Natl. Acad. Sci. U.S.A. 73*, 3862–3866.

Mendelsohn, R., & Maisano, J. (1978) *Biochim. Biophys. Acta 506*, 192–201.

Mendelsohn, R., & Tarashi, T. (1978) *Biochemistry 17*, 3944–3949.

Mendelsohn, R., & Koch, C. C. (1980) *Biochim. Biophys. Acta 598*, 260–271.

Mendelsohn, R., Sunder, S., & Bernstein, H. J. (1976) *Biochim. Biophys. Acta 443*, 613–617.

Mendelsohn, R., Anderle, G., Jaworsky, M., Mantsch, H. H., & Dluhy, R. A. (1984) *Biochim. Biophys. Acta 775*, 215–224.

Ohnishi, S. I. & Ito, T. (1974) *Biochemistry 13*, 881–887.

Papahadjopoulos, D., & Poste, G. (1975) *Biophys. J. 15*, 945–948.

Papahadjopoulos, D., Vail, W. J., Jacobson, D., & Poste, G. (1975) *Biochim. Biophys. Acta 394*, 483–491.

Pearson, R. H., & Pascher, I. (1979) *Nature (London) 281*, 499–501.

Petersen, N. O., Kroon, P. A., Kainosho, M., & Chan, S. I. (1975) *Chem. Phys. Lipids 14*, 343–349.

Pézolet, M., Duchesneau, L., Bougis, P., Faucon, J. F., & Dufourcq, J. (1982) *Biochim. Biophys. Acta 704*, 515–523.

Pézolet, M., Boulé, B., & Bourque, D. (1983) *Rev. Sci. Instrum. 54*, 1364–1367.

Poste, G., & Allison, A. C. (1973) *Biochim. Biophys. Acta 300*, 421–465.

Savitsky, J. E., & Golay, J. E. (1964) *Anal. Chem. 36*, 1627–1639.

Savoie, R., Boulé, B., Genest, G., & Pézolet, M. (1979) *Can. J. Spectrosc. 24*, 112-117.
Silvius, J. R., & Gagné, J. (1984a) *Biochemistry 23*, 3232-3240.
Silvius, J. R., & Gagné, J. (1984b) *Biochemistry 23*, 3241-3247.
Snyder, R. G., & Scherer, J. R. (1979) *J. Chem. Phys. 71*, 3221-3228.
Snyder, R. G., Hsu, S. L., & Krimm, S. (1978) *Spectrochim. Acta, Part A 34A*, 395-406.
Snyder, R. G., Scherer, J. R., & Gaber, B. P. (1980) *Biochim. Biophys. Acta 601*, 47-53.
Spiker, R. C., Jr., & Levin, I. W. (1975) *Biochim. Biophys. Acta 338*, 361-373.
Susi, H. (1981) *Chem. Phys. Lipids 29*, 359-368.
Van Dick, P. W. M., de Kruijff, B., Verkleij, A. J., Van Deenen, L. L. M., & de Gier, J. (1978) *Biochim. Biophys. Acta 512*, 84-96.
Verkleij, A. J., de Kruijff, B., Ververgaert, P. H. J. Th., Tocanne, J. F., & Van Deenen, L. L. M. (1974) *Biochim. Biophys. Acta 339*, 432-437.
Verkleij, A. J., de Maagd, R., Leunissen-Bijvelt, J., & de Kruijff, B. (1982) *Biochim. Biophys. Acta 684*, 255-262.

Flexibility of the Molecular Forms of Acetylcholinesterase Measured with Steady-State and Time-Correlated Fluorescence Polarization Spectroscopy†

Harvey Alan Berman,*,‡ Juan Yguerabide,§ and Palmer Taylor‡

Division of Pharmacology, Department of Medicine, and Department of Biology, University of California, San Diego, La Jolla, California 92093

Received October 4, 1984

ABSTRACT: Steady-state and time-correlated fluorescence polarizations have been examined for selected complexes and covalent conjugates of the 11S and (17 + 13)S forms of *Torpedo* acetylcholinesterase. The 11S form exists as a tetramer of apparently identical subunits, whereas the (17 + 13)S forms contain two or three sets of tetramers disulfide-linked to an elongated collagen-like tail unit. Pyrenebutyl methylphosphonofluoridate and (dansylsulfonamido)pentyl methylphosphonofluoridate were conjugated at the active center serine whereas propidium was employed as a fluorescent ligand for the spatially removed peripheral anionic site. Steady-state polarization of the pyrenebutyl conjugates indicates rotational correlation times of approximately 400 ns for the 11S species and greater than 1100 ns for the (17 + 13)S species. Hence, the tail unit severely restricts rotational motion of the catalytic subunits. Time-correlated fluorescence polarization analysis of the 11S species indicates multiple rotational correlation times. Anisotropy decay of the propidium complex (τ = 6 ns) occurs in exponential manner with a rotational correlation time of $\sim$150 ns, while covalent adducts at the active center exhibit rotational correlation times $\geq$300 ns. Anisotropy decay of the (dansylsulfonamido)pentyl conjugate (τ = 16 ns) appears exponential with a correlation time of approximately 320 ns, whereas decay of the pyrenebutyl conjugate (τ = 100 ns) is described by two correlation times, ϕ_S = 18 ns and ϕ_L = 320 ns, of small (15%) and large (85%) amplitudes, respectively. Two limiting models have been considered to explain the results. The first model considers the 11S form to behave as a *rigid* ellipsoid of revolution, whereas the second model incorporates the capacity for *segmental motion*. The biphasic decay seen with the longer lived probe and the differences in anisotropy decay seen for propidium and the active site ligands support the second model which incorporates protein flexibility.

Acetylcholinesterase (AchE)[1] can be isolated from electric organs of *Torpedo* as distinct molecular forms differing in molecular weight and complexity of structure (Lwebuga-Mukasa et al., 1976; Reiger et al., 1976; Viratelle & Bernhard, 1980; Bon & Massoulié, 1980; Lee et al., 1982a,b; Lee & Taylor, 1982). The 13S and 17S forms exist as large assemblies comprising two and three tetramers of catalytic subunits of 70000 daltons covalently associated through disulfide linkages with a collagenase-sensitive, filamentous tail unit and a noncollagenous subunit. The tail unit can be detected in electron micrographs as an elongated entity of 20 Å in diameter and 500 Å in length. Light tryptic digestion removes the noncollagenous and collagenous structural subunits, yielding an 11S species. The 11S or "lytic" form of acetylcholinesterase can be isolated as a tetrameric assembly comprised of four apparently equivalent subunits of 70000 daltons. As deduced from its frictional coefficient of 1.65, the 11S AchE species exhibits substantial dimensional asymmetry (Taylor et al., 1974). The catalytic subunits on the 11S and the tail-con-

† Supported by USPHS Grant GM-18360 to P.T., USPHS Grant ES-03085, and a grant from the U.S. Army Research Office to H.A.B.

* Address correspondence to this author at the Department of Biochemical Pharmacology, School of Pharmacy, State University of New York at Buffalo, Buffalo, NY 14260.
‡ Division of Pharmacology, Department of Medicine.
§ Department of Biology.

[1] Abbreviations: AchE, acetylcholinesterase; PBMP-AchE, (pyrenebutyl methylphosphono)acetylcholinesterase; DC_5MP-AchE, [(dansylsulfonamido)pentyl methylphosphono]acetylcholinesterase; PBMPF, pyrenebutyl methylphosphonofluoridate; Tris-HCl, tris(hydroxymethyl)aminomethane hydrochloride.

0006-2960/85/0424-7140$01.50/0